Abstract number: 2017-306
2017 INTERNATIONAL OIL SPILL CONFERENCE

TITLE: PREDICTION OF OIL DROPLET MOVEMENT AND SIZE DISTRIBUTION: LAGRANGIAN METHOD AND VDROP-J MODEL

AUTHORS: Feng Gao[1], Lin Zhao[1], Frank Shaffer[2], Roozbeh Golshan [1], Michel Boufadel[1*], Thomas King[3], Brian Robinson[3], Kenneth Lee[3]

Affiliation of authors:

1: Center for Natural Resources Development and Protection, Department of Civil and Environmental Engineering, New Jersey Institute of Technology, Newark, NJ, United States

2: National Technology Energy Lab, Department of Energy, Morgantown, WV, United States

3: Bedford Institute of Oceanography, Department of Fisheries and Oceans, Dartmouth, NS, Canada

Mailing address of authors:

1: Colton Hall, New Jersey Institute of Technology, 323 MLK Blvd, Newark, NJ, United States, 07102-1824

2: 3610 Collins Ferry Road, P.O. Box 880, Morgantown, WV, United States, 26507

3: Bedford Institute of Oceanography, P.O. Box: 1006, Dartmouth, NS, B2Y 4A2, Canada

*Corresponding author. E-mail address: boufadel@gmail.com (M.C. Boufadel).

ABSTRACT (2017-306):

During subsurface oil releases, oil disperses into droplets whose trajectories depend on the droplet size. We report the measurements of the droplet size distribution (DSD) obtained from the release of diesel at 135 GPM from a horizontal pipe in the Ohmsett tank. The DSD was predicted using the model VDROP-J and matched the observation. Subsequently, the movement of the droplets was tracked using a Lagrangian Particle Tracking (LPT) approach. Various forces affecting the migration of the droplets were considered, these include drag, buoyancy, lift, and added mass force. It was found that the lift force is negligible. The added mass force was negligible for droplets smaller than 500 μm.

Visual observation and modeling indicated that large droplets (larger than 300 μm) tend to separate from the plume and migrate upward independently, which affects, not only the DSD of large droplets but also the resulting daughter droplets. This is an issue that has not been addressed in the literature. Our findings indicate that the DSD is needed to better predict the trajectory of oil blowouts.

INTRODUCTION

Jets and plumes of oil and gas could be encountered following underwater releases due to oil and gas operations. Other cases include underwater hydrothermal-vents (Norman and Revankar, 2010), wastewater discharge from outfalls (Hunt et al., 2010), production and transportation (Bosanquet et al., 1961). Underwater oil jets/plumes have gained more attention from researchers after the disastrous the oil spill from Deepwater Horizon Blowout in 2010 with more than 200 million gallons of crude oil released into the Gulf of Mexico (NRC, 2003; Ramseur, 2010). The mitigation of oil spills depends on the trajectory and fate

of oil droplets. This requires understanding the mechanisms that generate the droplets (oil dispersion including breakup and coalescence of droplets) and the mechanisms that affect their trajectories. Dissolution would tend to reduce the size of the droplets, but not in a major way. Emulsification and biodegradation tend to occur after days, while dispersion from blowouts occurs over seconds to minutes.

Extensive studies show that the transport and fate of oil are greatly affected by the droplet size (Brakstad et al., 2015; Chen et al., 2015; Ramseur, 2010). There is an increase of surface area due to the increasing number of small droplets, a larger surface area enhances the dissolution of hydrocarbon and oil biodegradation subsequently (Zhao et al., 2016). Small droplets have low buoyancy (Geng et al., 2016) such that they are more likely to remain underwater suspended by turbulence, while large droplets tend to rise to the water surface rapidly (Korotenko et al., 2004). Droplets with smaller sizes are more subject to the influence of turbulence compared to larger ones (Wang et al., 2016). Although various models (Chen and Yapa, 2004; Johansen, 2000; Zhao et al., 2015; Zheng et al., 2003) and field experiments (Chen and Yapa, 2003; Johansen et al., 2003; Zhao et al., 2016) were carried out to study the impact and physics of oil spills, few of them have considered the comprehensive forces exerted on the droplets which may influence the movement of single oil droplets under turbulence.

In the present study, we performed an underwater oil release experiment in the Ohmsett tank from a 1.0 inch horizontal pipe. The oil droplet size distribution was measured using LISST and predicted using the model VDROP-J (Zhao et al., 2014a) and used a Lagrangian Particle Tracking (LPT) model to trace the trajectories of individual droplets. We accounted for the impact of turbulence and the forces due to drag, buoyancy, added mass, and lift, which were obtained from computational fluid dynamics (CFD) simulation. We also

evaluated the relative importance of different forces for single droplets with different diameters. The experiment and simulations were of dead oil (i.e., no gas dissolved in the oil).

EXPERIMENTAL SETUP

The release of oil was from a horizontal orifice in the Ohmsett tank in New Jersey. The tank is 203 m long, 20 m wide, and 3.4 m tall, but contained water at a depth of 2.4 m. The orifice was 1.3 m above the bottom of the tank with a diameter of 25.4 mm. A high resolution camera was placed at the downstream of the jet to capture the overall oil plume trajectory. A schematic view of the horizontal oil jet experiment is shown in Figure 1.

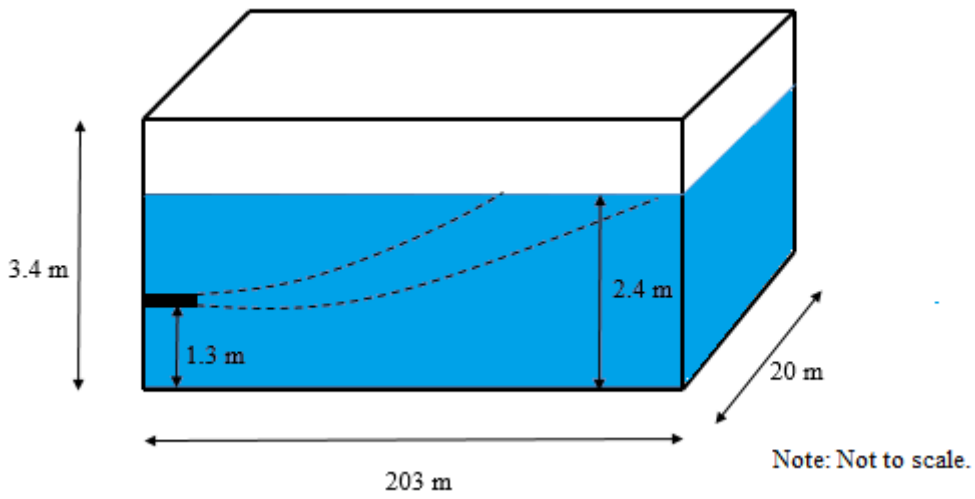

Figure 1: The schematic view of the horizontal oil jet.

The oil used in the experiment was JP5 whose density ρ_o = 820 kg/m^3, dynamic viscosity μ_o=4.38 cp, and interfacial tension with water σ=0.02 N/m. The oil injection flow rate (Q) was 135 GPM. Based on the volumetric oil flow rate and the diameter of the orifice, the average oil exit velocity from the orifice (U_o) was 16.8 m/s.

NUMERICAL IMPLEMENTATION

(1) Computational Fluid Dynamics (CFD)

The hydrodynamics of the plume was modeled using Reynolds Averaged Navier Stokes (RANS) model within the commercial CFD software ANSYS Fluent®. RANS model has been successfully used in a wide range of engineering applications to predict the average turbulent characteristics (Bo et al., 2017; Gao et al., 2017). And we used these quantities within a Lagrangian Particle Tracking (LPT) method to predict the oil droplet trajectories, which is detailed in following section.

(2) Lagrangian Particle Tracking (LPT)

The movement of each droplet is determined by solving a set of ordinary differential equations along its path. This approach is suitable to model two phase flows with relative low particle concentration with non-uniform properties (Joao et al. 2010), as in the present work. The equations for calculating the oil droplet location are defined in the following (Geng et al., 2014):

$$X_d' = X_d + U_d \Delta t + R\sqrt{2D\Delta t} \quad (1)$$

where X_d' is the coordinates of the droplet at the next time level. X_d and U_d are the coordinates and velocity of the oil droplets at the current time level, respectively, which are given as $X_d = (x, y, z)_d$ and $U_d = (\mathrm{u}, \mathrm{v}, \mathrm{w})_d$. The subscript "*d*"denotes droplet. The third term on the RHS of Eq. (1) represents the impact of turbulence on the subscale movement of the oil droplet, which is accounted for by using a random walk process, where R represents a random number generated from Gaussian distribution with a mean of 0 and a variance of 1.0. Δt is time step. D is eddy diffusivity, which is calculated as:

$$D = 0.09\frac{k^2}{\varepsilon} \tag{2}$$

in which k is turbulence kinetic energy and ε is turbulence dissipation rate, both are obtained CFD (e.g., RANS model) described above.

The oil droplets are subject to comprehensive forces based on Newton Second Law:

$$m_o \frac{d}{dt}(U_d) = F_g + F_b + F_l + F_a + F_d \tag{3}$$

m_o is the mass of oil droplet. All relevant forces are expressed on the RHS of Equation (3): F_g is gravitational force, F_b is buoyancy force due to oil droplet and water density difference, F_l is lift force, F_a is added mass force, and F_d is drag force. The Basset force is known as the history term, and is negligible herein as noted in prior works by Sridhar and Katz (1995). The gravitational force F_g is given by the following assuming oil droplet is of spherical shape:

$$F_g = \frac{1}{6}\pi\rho_o D_d^3 g \tag{4}$$

where ρ_o is oil density, $\mathrm{D_d}$ is droplet diameter and g is gravity. The gravity force points downward and is assigned as positive. The buoyancy force due to the density difference between oil droplets and surrounding liquid is given by:

$$F_b = -\frac{1}{6}\pi\rho_w D_d^3 g \tag{5}$$

where ρ_w is water (continues phase) density, taken as 998.2 $\mathrm{kg/m^3}$ in the present study.

F_l is expressed as follows (Joao Pinto, 2010):

$$F_l = \frac{\pi}{8}\rho_w D_d^3 C_l\left[(U - U_d)\times\omega\right] \tag{6}$$

in which ρ_w is water (continuous phase) density, U is the local velocity of the surrounding water (continuous phase). D_d is oil droplet diameter, C_l is lift coefficient, which usually varies between 0.01 for very viscous fluid and 0.5 for inviscid fluid (Burlutskiy and Turangan, 2015). We take C_l as 0.1 in the present study. ω is vorticity and reads as:

$$\omega = \nabla \times U \tag{7}$$

F_a accounts for the acceleration of oil droplet due to its movement through the surrounding water volume, which is expressed as the following (Tomiyama, 1998):

$$F_a = C_a m_w \left(\frac{dU}{dt} - \frac{dU_d}{dt} \right) \tag{8}$$

with $C_a = 0.5$, taken as a constant (Lucas et al., 2005) and m_w is the mass of water taking the same volume as the oil droplet. F_d accounts for the resistance acting in the opposite direction of moving oil droplet with respect to water (Miller et al., 1998):

$$F_d = \frac{f_d}{\tau_d}(U - U_d) m_o \tag{9}$$

where m_o is the mass of oil droplet and τ_d is the Stokes drag coefficient given as:

$$\tau_d = \frac{\rho_o * D_d^{\,2}}{18 * \mu_o} \tag{10}$$

The variable of f_d is a correction for the Stokes coefficient to account for situations where the flow is not laminar, which is calculated based on Miller et al. (1998):

$$f_d = 1 + 0.0545 \mathrm{Re}_d + 0.1\sqrt{\mathrm{Re}_d}\,(1 - 0.03\mathrm{Re}_d) \tag{11}$$

where Re_d are defined as follows:

$$\mathrm{Re}_d = \frac{\rho_w D_d \mathrm{u}_s}{\mu_w} \tag{12}$$

where μ_w is water dynamics viscosity and u_s is slip velocity.

We incorporated Equations (4)-(12) into Equation (3) using single step forward Euler scheme for time stepping. The Inverse Distance Weighted Method (IDVM) was used to interpolate the local flow velocity in space, to obtain the velocity of the particle:

$$\mathrm{U}_j(x_d, y_d, z_d) = \sum_{i=0}^{N} \frac{\theta_i \mathrm{U}_{ji}}{\sum_{j=0}^{N} \theta_i \mathrm{U}_{ji}}, \ \theta_i(x) = \frac{1}{d^p}, \ j = x, y, z \tag{13}$$

where *d* is the distance from the oil droplet position to the nodes of the CFD domain where the velocity of water is provided. The term *p* is a selected power, which is normally taken as 2.0.

(3) VDROP-J Model

The droplet size distribution (DSD) was modeled using VDROP-J, which was developed by combining the transient droplet size distribution with hydrodynamic correlations of jets and plumes (Zhao et al., 2014b; Zhao et al., 2014c). The mechanism of breakup dominates droplet formation as the holdup of oil dramatically decreases once the oil is released from the orifice. An important parameter in the model VDROP-J is the breakup coefficient Kb calculated as:

$$Kb = 3.57(\rho_o U_0^2 D_0)^{-0.63} \tag{14}$$

where ρ_o is the oil density. U_0 and D_0 are the initial jet velocity and orifice diameter.

RESULTS AND DISCUSSION

Figure 3 shows the oil plume profile by using the high resolution camera in the experiment under steady state condition. The dotted and solid black lines indicate the plume boundary and the centerline predicted by the JETLAG model (Cheung and Lee, 1990). The lower boundary of the oil plume from the experiment and JETLAG model agreed quite well, however, JETLAG undershot the upper boundary of the oil plume. As shown in Figure 3, some droplets reached the upper boundary of the plume obtained from JETLAG model and continue to rise up to exit the plume, which indicates that the movement of large droplets is different from that of the plume. It is possible that the buoyancy of larger diameter droplet is large enough to overcome the turbulence mixing energy while small ones are more likely to be more uniformly mixed within the oil plume. Figure 3 substantiates the necessity to account for the rise of individual droplets by considering the physical forces.

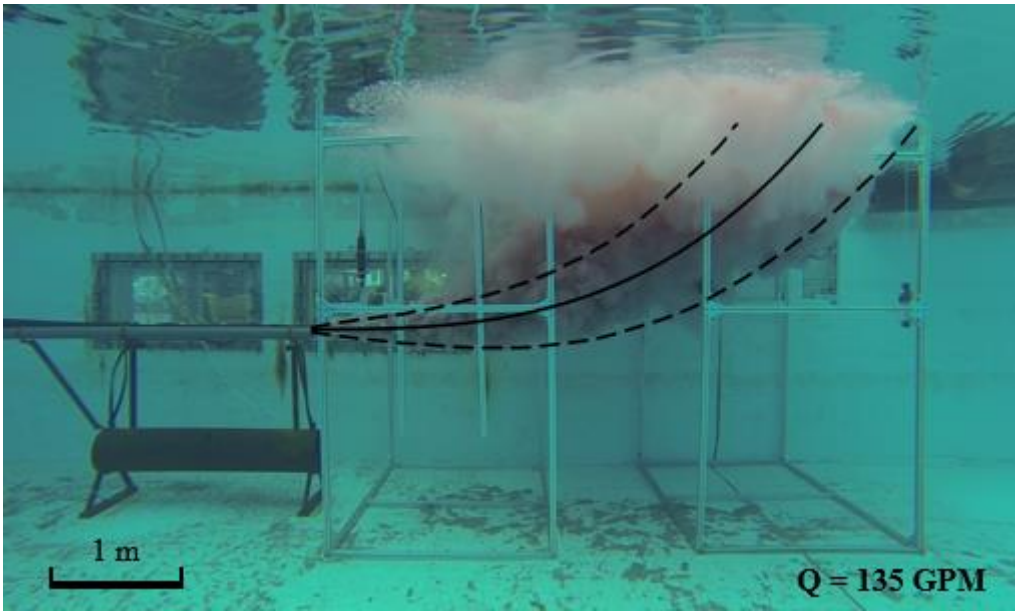

Figure 3: The profile of oil release experiment (Q=135 GPM) under steady state. The dotted and solid black lines are the plume boundary and centerline predicted by JETLAG model, respectively.

Figure 4 shows the time series of vertical component of physical forces (F_o , e.g., buoyancy force, lift force, drag force, added mass force) over droplets of different diameters. Note that the physical forces were scaled by gravitational force. The scaled buoyancy force is a straight-line with no mass transport and maintains constant oil droplet density. The added mass force is almost negligible for droplets less than 500 μm in diameter, as shown in Figure 4a and 4b. Even for large droplets with 500 μm in diameter, the added mass force is around 17 % of buoyancy force of droplet, as shown in Figure 4c. The scaled lift force is negligible although it slightly increases as droplet diameter is increased to 500 μm . Figure 4 indicates that the main contributing forces in the process of oil droplet rising are the buoyancy force and the drag force.

Figure 5a shows the comparison between experimental and VDROP-J model results of Droplet size distribution (DSD). The distribution peak was located that 237.8 and 461 in the experimental measurement. Oil droplets mostly occupied the volume with the larger size. The VDROP-J model was configured with the experimental conditions for jet diameter, oil and tank water properties (e.g. viscosity, density, and interfacial tension) and discharge rates. The LISST detected the largest droplet size of 461 μm during the experiment, which is the upper limit of the instrument detection. By calibration with experimental data, the initial oil droplet size was assumed to consist only of droplets with size 700 μm. Droplet sizes were discretized into 140 classes with 5 μm increment for each size bin to minimize discretization errors.

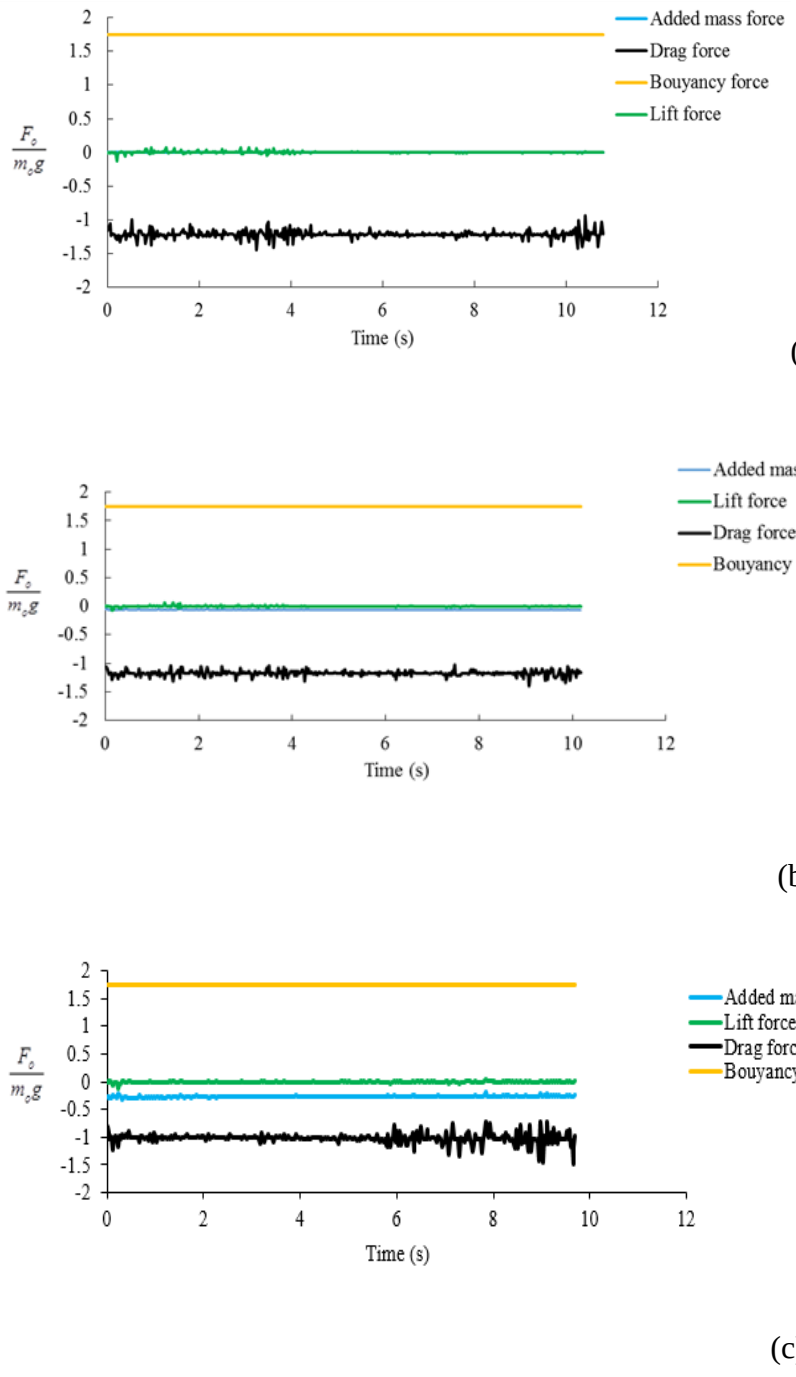

Figure 4: Time series of vertical component of the physical forces over a single droplet (a) 50 μm in diameter (b) 200 μm in diameter (c) 500 μm in diameter. Note the physical forces are scaled by gravity.

Since experimental data obtained from LISST were for droplets up to 461 μm, a comparison between predictions and measurements were made only in this range. The modeling results (the column of model predictions in Figure 5) were obtained at 4.3 m downstream distance from the jet exit, which equals an approximate distance from jet exit to the device subject to plume trajectories. Predicted data were in uniform size bins (with 5 μm increment from 5 μm to 700 μm) and regrouped into the size bins of the experimental data (e.g. the summation of predicted volume in bins of 145-170 μm is compared with the experimental data in the bin of 170.8 μm) as shown in Figure 5. The overall agreement between VDROP-J model and the LISST experimental data was quite good, especially for oil droplet size up to 280.6 μm. There was a relative larger discrepancy between LISST and VDROP-J model results at smaller (e.g. less than 74.65 μm) and larger (e.g., 331.1 μm) sized droplets. The discrepancy is possibly because the LISST measurement started 3 s after the injection stopped such that some of the large droplets resurfaced quickly and were not captured by the LISST. However, a more likely reason for the discrepancy is that large oil droplets tend to rise up and exit the plume boundary, which was observed in Figure 3, and thus few oil droplets were captured by LISST measurement.

Figure 5b shows a full range droplet size distribution from VDROP-J model at the LISST location. A bi-modal distribution is observed, with peaks at 280 μm and 515 μm. The predicted d_{50} value is 310 μm. Larger sized droplets were not measured by LISST due to the limitation of the instrument detection, however, the DSD of larger sized droplets were predicted by VDROP-J model.

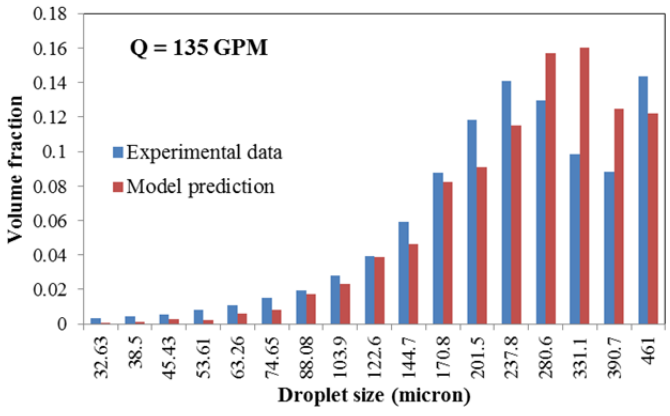

(a)

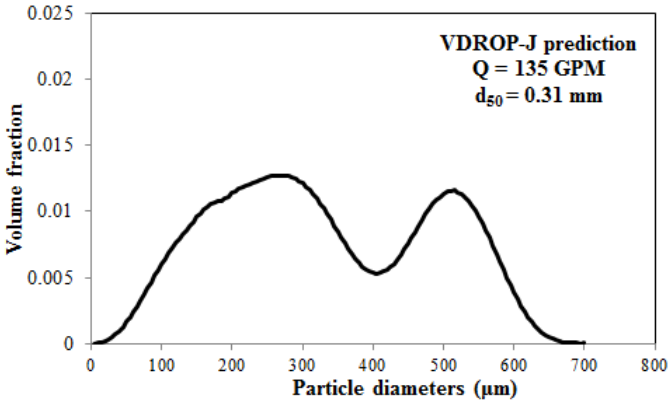

(b)

Figure 5: Droplet size distribution (DSD) obtained from the in situ monitoring LISST and VDROP-J model (a) comparison between LISST measurement and VDROP-J model results (b) full-range modeling predictions of VDROP-J. The experimental data was the average of 5 data points after the saturation of LISST. Modeling results were obtained from VDROP-J model at 4.3 m downstream distance from the jet exit, which is an approximate location of the LISST subject to the plume. We matched the LISST results for sizes smaller than 461 μm, and we used the model VDROP-J to predict the larger sizes.

CONCLUSIONS

In the present study, we studied the oil plume profile from subsurface oil release experiment by using high resolution camera. It was observed that some oil droplets exited the boundary of the plume and continue to rise up depending on its own buoyancy while most droplets stay within the oil plume, which is possibly because larger oil droplets have larger buoyancy to overcome the turbulence mixing energy while smaller ones are more likely be to uniformly mixed within the oil plume. The experimental observation further substantiated the necessity to account for the individual droplets movement by considering the comprehensive physical forces on the droplet.

We introduced a Lagragian particle tracking (LPT) model that coupled with Computational Fluid Dynamics (CFD) simulation by considering the comprehensive forces on oil droplets of different diameters, including gravitational force, buoyancy, lift force, drag force and added mass force. The relative importance of different forces was evaluated by Lagrangian Particle Tracking (LPT) model and was concluded that the two main contributing forces are buoyancy and drag force. The added mass force becomes more important when droplet size is large (e.g., 500 μm) while lift force is negligibly small.

The droplet size distribution (DSD) from LISST measurement was compared with the numerical simulation results by VDROP-J. The overall agreement was quite good, especially for the medium sized oil droplets, while the discrepancy was larger at smaller (e.g. less than 74.65 μm) and larger (e.g., 331.1 μm) sized droplets, which is most possibly because large droplets tend to rise up with a larger buoyancy and exit the boundary of the plume, and thus fewer large oil droplets were captured by LISST in the experiment.

REFERENCES

Bo, Z., Chao, Z., Zhiming, J., and Chao-Hsin, L., 2017, Design and characterization of a cough simulator: Journal of Breath Research, v. 11, no. 1, p. 016014.

Bosanquet, C. H., Horn, G., and Thring, M. W., 1961, The Effect of Density Differences on the Path of Jets: Proceedings of the Royal Society of London A: Mathematical, Physical and Engineering Sciences, v. 263, no. 1314, p. 340-352.

Brakstad, O. G., Nordtug, T., and Throne-Holst, M., 2015, Biodegradation of dispersed Macondo oil in seawater at low temperature and different oil droplet sizes: Marine Pollution Bulletin, v. 93, no. 1–2, p. 144-152.

Burlutskiy, E., and Turangan, C. K., 2015, A computational fluid dynamics study on oil-in-water dispersion in vertical pipe flows: Chemical Engineering Research and Design, v. 93, p. 48-54.

Chen, F., and Yapa, P. D., 2003, A model for simulating deep water oil and gas blowouts - Part II: Comparison of numerical simulations with "Deepspill" field experiments: Journal of Hydraulic Research, v. 41, no. 4, p. 353-365.

Chen, F., and Yapa, P. D., 2004, Three-dimensional visualization of multi-phase (oil/gas/hydrate) plumes: Environmental Modelling & Software, v. 19, no. 7–8, p. 751-760.

Chen, H., An, W., You, Y., Lei, F., Zhao, Y., and Li, J., 2015, Numerical study of underwater fate of oil spilled from deepwater blowout: Ocean Engineering, v. 110, Part A, p. 227-243.

Cheung, V., and Lee, J. H. W., 1990, Generalized Lagrangian Model for Buoyant Jets in Current: Journal of Environmental Engineering, v. 116, no. 6, p. 1085-1106.

Gao, F., Shoai Naini, S., Wagner, J., and Miller, R., 2017, An experimental and numerical study of refrigerator heat leakage at the gasket region: International Journal of Refrigeration, v. 73, p. 99-110.

Geng, X., Boufadel, M. C., Ozgokmen, T., King, T., Lee, K., Lu, Y., and Zhao, L., 2016, Oil droplets transport due to irregular waves: Development of large-scale spreading coefficients: Marine pollution bulletin, v. 104, no. 1, p. 279-289.

Geng, X., Boufadel, M. C., Xia, Y., Li, H., Zhao, L., Jackson, N. L., and Miller, R. S., 2014, Numerical study of wave effects on groundwater flow and solute transport in a laboratory beach: Journal of Contaminant Hydrology, v. 165, p. 37-52.

Hunt, C. D., Mansfield, A. D., Mickelson, M. J., Albro, C. S., Geyer, W. R., and Roberts, P. J. W., 2010, Plume tracking and dilution of effluent from the Boston sewage outfall: Marine Environmental Research, v. 70, no. 2, p. 150-161.

Joao Pinto, Y. F., Luis Oliveira, Christian Tenaud, 2010, Numerical simulaiton of a two-phase flow in an oil filter couplilng a LES approach with a Lagrangian particle tracking V European Conference on Computational Fluid Dynamics ECCOMAS CFD 2010: Lisbon, Portugal.

Johansen, Ø., 2000, DeepBlow – a Lagrangian Plume Model for Deep Water Blowouts: Spill Science & Technology Bulletin, v. 6, no. 2, p. 103-111.

Johansen, Ø., Rye, H., and Cooper, C., 2003, DeepSpill—Field Study of a Simulated Oil and Gas Blowout in Deep Water: Spill Science & Technology Bulletin, v. 8, no. 5–6, p. 433-443.

Korotenko, K. A., Mamedov, R. M., Kontar, A. E., and Korotenko, L. A., 2004, Particle tracking method in the approach for prediction of oil slick transport in the sea: modelling oil pollution resulting from river input: Journal of Marine Systems, v. 48, no. 1–4, p. 159-170.

Lucas, D., Prasser, H. M., and Manera, A., 2005, Influence of the lift force on the stability of a bubble column: Chemical Engineering Science, v. 60, no. 13, p. 3609-3619.

Miller, R. S., Harstad, K., and Bellan, J., 1998, Evaluation of equilibrium and non-equilibrium evaporation models for many-droplet gas-liquid flow simulations: International Journal of Multiphase Flow, v. 24, no. 6, p. 1025-1055.

Norman, T. L., and Revankar, S. T., 2010, Jet-plume condensation of steam–air mixtures in subcooled water, Part 1: Experiments: Nuclear Engineering and Design, v. 240, no. 3, p. 524-532.

NRC, 2003, Oil in the sea III: inputs, fates, and effects, National Research Council, National Academies Press: Washington, D.C.

Ramseur, J. L., 2010, Deepwater Horizon Oil Spill: The Fate of the Oil Congressional Research Service

Sridhar, G., and Katz, J., 1995, Drag and lift forces on microscopic bubbles entrained by a vortex: Physics of Fluids, v. 7, no. 2, p. 389-399.

Tomiyama, A., 1998, Struggle with computational bubble dynamics, Third International Conference on Multiphase Flow, ICMF ’98: Lyon, France.

Wang, Z., DiMarco, S. F., and Socolofsky, S. A., 2016, Turbulence measurements in the northern gulf of Mexico: Application to the Deepwater Horizon oil spill on droplet dynamics: Deep Sea Research Part I: Oceanographic Research Papers, v. 109, p. 40-50.

Zhao, L., Boufadel, M. C., Adams, E., Socolofsky, S. A., King, T., Lee, K., and Nedwed, T., 2015, Simulation of scenarios of oil droplet formation from the Deepwater Horizon blowout: Marine Pollution Bulletin, v. 101, no. 1, p. 304-319.

Zhao, L., Boufadel, M. C., Adams, E. E., Socolofsky, S. A., and Lee, K., A Numerical Model for Oil Droplet Evolution Emanating from Blowouts, *in* Proceedings International Oil Spill Conference Proceedings, Savannah Georgia, USA, 2014a, Volume 2014, American Petroleum Institute, p. 561-571.

Zhao, L., Boufadel, M. C., Socolofsky, S. A., Adams, E., King, T., and Lee, K., 2014b, Evolution of droplets in subsea oil and gas blowouts: Development and validation of the numerical model VDROP-J: Marine Pollution Bulletin, v. 83, no. 1, p. 58-69.

Zhao, L., Shaffer, F., Robinson, B., King, T., D'Ambrose, C., Pan, Z., Gao, F., Miller, R. S., Conmy, R. N., and Boufadel, M. C., 2016, Underwater oil jet: Hydrodynamics and droplet size distribution: Chemical Engineering Journal, v. 299, p. 292-303.

Zhao, L., Torlapati, J., Boufadel, M. C., King, T., Robinson, B., and Lee, K., 2014c, VDROP: A comprehensive model for droplet formation of oils and gases in liquids - Incorporation of the interfacial tension and droplet viscosity: Chemical Engineering Journal, v. 253, p. 93-106.

Zheng, L., Yapa, P. D., and Chen, F., 2003, A model for simulating deepwater oil and gas blowouts - Part I: Theory and model formulation: Journal of Hydraulic Research, v. 41, no. 4, p. 339-351.